

*Dr. R. Temirov*

*Peter Grünberg Institut 3, Forschungszentrum Jülich*

## **Versuch:**

# **Low Temperature Scanning Tunnelling Microscopy and Spectroscopy in Ultrahigh Vacuum**

## **1 Introduction**

Scanning probe microscopy has become an essential tool in the field of nano-science to perform local experiments on the atomic scale. The scanning tunnelling microscopy is a widely used technique to obtain surface morphology of conducting samples down to atomic resolution. However, the method is not limited to the topography only but gives many possibilities to study ultra small objects like molecules and atoms. For example, in a scanning tunnelling microscope (STM) one can manipulate single molecules or even atoms at surface, measure energy levels of electrons in an adsorbed molecule or image electron wave function in a quantum dot (artificial atom), make current measurements through a single molecule or chain of atoms and many other things.

Especially interesting experiments can be done at low temperatures (approximately 5 K). The low temperature ensures a very high electrical and mechanical stability of the microscope, with a minimum of thermal drift in the instrument. Moreover, at these temperatures the diffusion of atoms and molecules on the sample surface is strongly suppressed, and the smearing of the Fermi distribution which limits the energy resolution in scanning tunnelling spectroscopy is reduced. It thus becomes possible to address single molecules and measure their electronic properties and vibrations with very high energy resolution. Single molecules or atoms can be manipulated on the substrate using the STM tip. In this way the nanostructures can be built atom by atom, or molecule by molecule. The experiments are performed under conditions of ultrahigh vacuum (UHV, pressures smaller than  $10^{-10}$  mbar) in order to prevent the adsorption of contaminants.

This practical training covers only a small (but most important) part of the scanning tunneling microscopy technique, in particular the topographic imaging and simple spectroscopic measurements.

## 2 Experimental Setup

### 2.1 Experimental system

The experimental setup of the Createc Low Temperature UHV STM used in this experiment is shown in *Fig.1*. The system has a base pressure  $P < 3 \times 10^{-11}$  mbar that allows to produce clean surfaces free of contaminations and keep them clean for extended time for the STM investigation.

The system comprises a load-lock chamber, preparation chamber, STM chamber and a set of vacuum pumps. The load-lock chamber is used to introduce and transfer the sample from air to the UHV part of the system. The sample is mounted on a specially designed sample holder on which the sample can be heated. Sample preparation (cleaning by ion bombardment and heating; material deposition) and in-situ tip preparation (heating) is carried out in the preparation chamber. The preparation chamber is equipped with coolable (liquid  $^4\text{He}$  flow cryostat) sample manipulator on which the sample holder is mounted during sample preparation, an ion gun for sample cleaning, a quadrupole mass spectrometer (QMS) for residual gas analysis, and several evaporators for the deposition of different materials. Prepared samples can be pre-cooled on the manipulator and transferred into the cold STM without exposition to air, thus preserving the surface for subsequent STM measurements with atomic resolution. The complete system is mounted on a metal frame and placed on a pneumatic vibration isolation system to reduce acoustic noise from the environment of the microscope.

### 2.2 Low temperature scanning tunnelling microscope

The cryostat and the scanning unit are shown schematically in *fig. 2*. The scanning unit is suspended on springs (for vibration insulation) from the bottom of the  $^4\text{He}$  bath cryostat ( $T=4.2$  K) and shielded from thermal radiation by a 4.2 K radiation shield. The  $^4\text{He}$  cryostat and the 4.2K radiation shield are surrounded by a tank of liquid nitrogen ( $T=77$  K) and a 77 K radiation shield. In this way the complete scanning unit (with sample holder, sample and tip) can be maintained at a temperature of approximately 5 K. For initial cooling, the scanning unit is pulled into contact with the 4.2 K shield.

The Createc scanning unit is an inverted beetle-type STM. It consists of a sector ramp with the z-piezo in the centre, and three outer piezos that are fixed on a base plate. The sector ramp rests under its own weight on sapphire balls that are glued to the outer piezos. The tip in its holder is attached to the centre z-piezo. The tip is made of tungsten. It is extremely sharp and ideally terminated by a single atom. The sample holder with the sample is pressed to the base plate from below, such that the sample surface faces the tip. For coarse approach, the outer piezos are actuated in such a way that the sector ramp rotates on the three sapphire balls. As a consequence, the z-piezo (and with it the tip) moves towards the sample. The outer piezos can also be actuated in such a way that the sector ramp slides sideways on the sapphire balls; in this way the lateral position of coarse approach can be chosen. Once the tip is in tunnelling contact to the sample, the tip-sample distance can be controlled by the extension of the z-piezo, while the lateral position of the tip relative to the sample can be controlled by bending of the z-piezo.

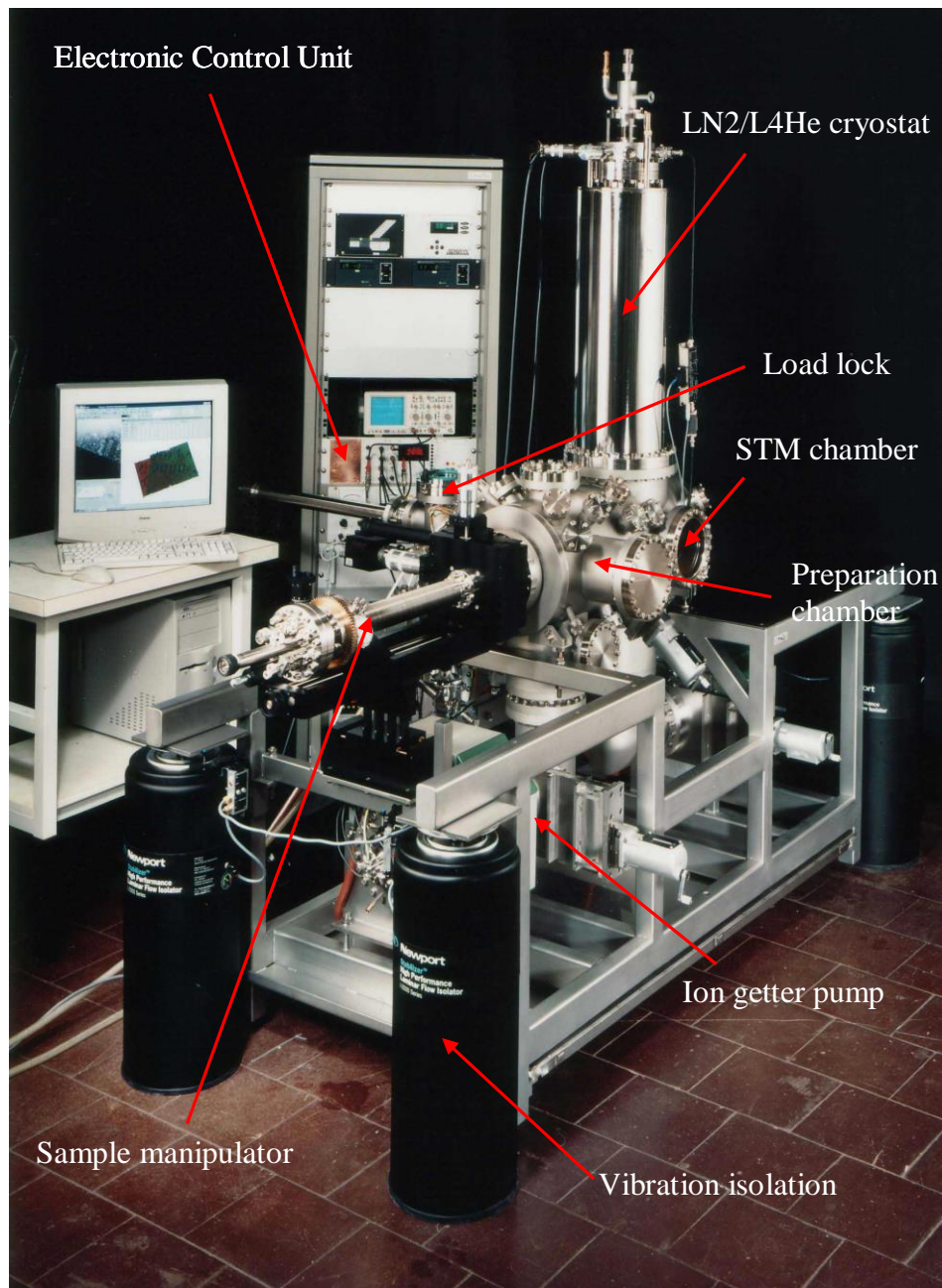


*Fig.1 Photograph of the experimental system (Createc STM).*

At separations of a few angstroms between the tip and substrate electrons become able to tunnel through the vacuum barrier via the quantum mechanical tunneling effect at a bias voltage applied between the tip and surface. The tunneling current is extremely sensitive to the distance between tip and sample due to the exponential decay of the electron wave functions inside the barrier. It provides a very good resolution perpendicular to the surface. Since the current falls off so rapidly with distance, most of the tunneling current flows through the apex atom of the tip giving lateral atomic resolution.

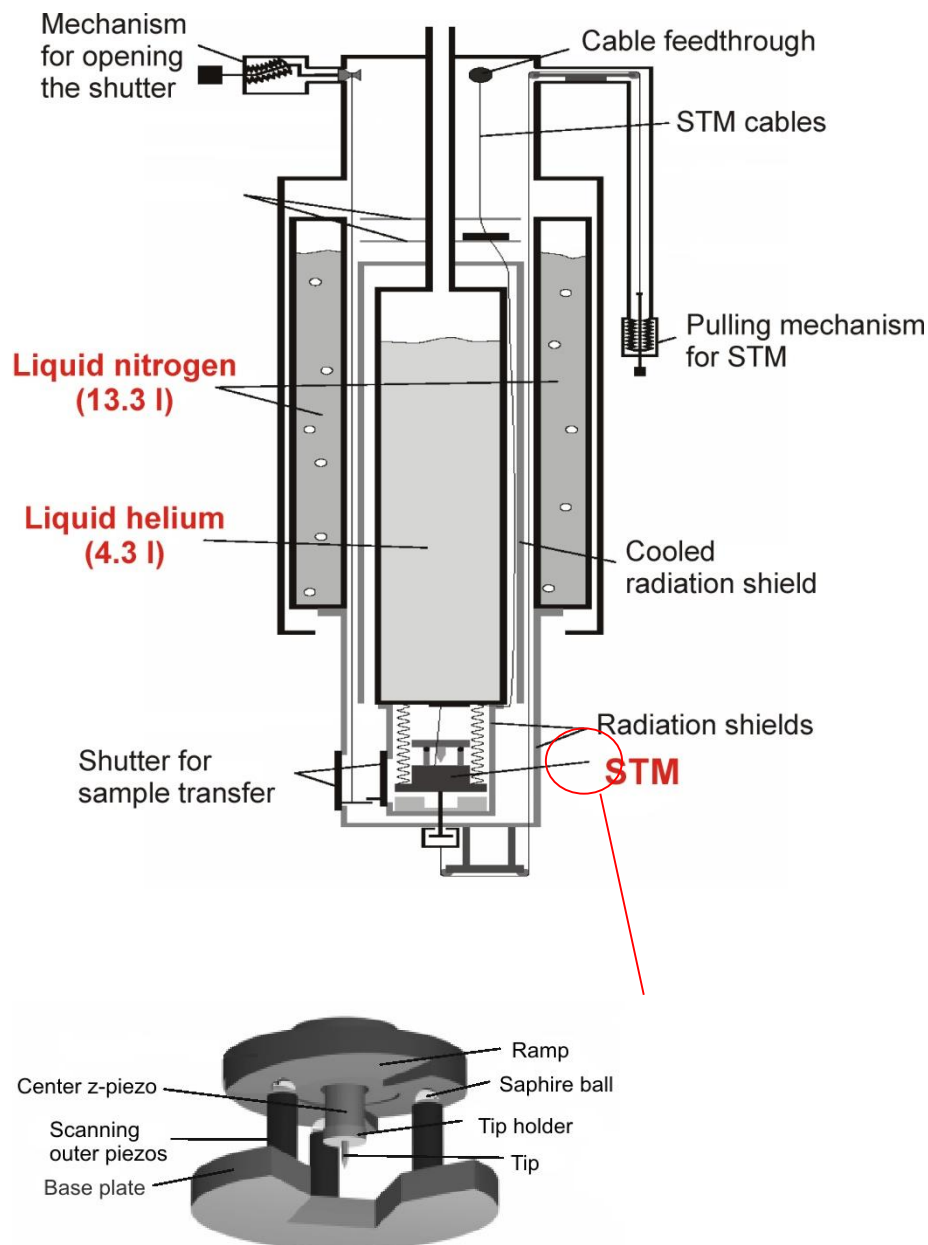


*Fig.2 Cryostat (top) and scanning unit (bottom) of the Createc scanning tunnelling microscope.*

### 3 Principles of Scanning Tunnelling Microscopy

#### 3.1 Quantum mechanical tunnelling in one dimension

Here we consider a one-dimensional approximation for one electron tunneling in order to grasp the very important exponential dependence of the tunneling current on the tip sample distance.

In quantum mechanics electrons in a solid are described by waves. The electrons which are responsible for charge transport in metals are the ones with the highest energy, close to the Fermi level. The energy of the electrons at the Fermi level ( $E_F$ ) is lower than the vacuum energy, due to the bonding of the electrons to the atom cores. The minimum energy needed to remove an electron from a solid to a point immediately outside the solid surface is called work function  $\phi$ .

Thus at a surface there is a barrier for the electrons to leave from the solid to the vacuum level  $E_{\text{vac}}$  (top panel of Fig. 3a). In classical mechanics particles cannot penetrate into a barrier which is higher than their energy. Quantum mechanically particles can penetrate to a region with a barrier higher than their energy. An ansatz with an exponentially decaying wave function inside the barrier (in the vacuum) leads to a solution of the Schroedinger equation for this potential barrier (Fig. 3a). The probability of a particle to be at a position  $z$  inside the barrier is proportional to  $|\psi(z)|^2$ ,

$$|\psi(z)|^2 = |\psi(0)|^2 e^{-2\kappa z}$$

$$\kappa = \sqrt{\frac{2m\phi}{\hbar^2}}$$

If after some distance  $d$  the vacuum is replaced by another solid this configuration is already a one-dimensional model of the tunneling junction (electrode-gap-electrode). A potential diagram for such a tunneling barrier is shown in Fig. 3(b). The wave function of a free electron in the second electrode is an oscillating wave again. The solution of the square barrier problem gives the transmission coefficient  $T$  for the wave function behind the barrier:

$$T = \frac{|\psi(d)|^2}{|\psi(0)|^2} \approx e^{-2\kappa d}$$

If the work functions of the solids are different the resulting barrier can be approximated by the average work function  $\phi = (\phi_{\text{tip}} + \phi_{\text{sample}})/2$ .

The transmission coefficient and therefore the tunneling probability decays exponentially with the tip sample distance  $d$  and the tunneling probability decreases exponentially with the square root of the work function. If we use one electrode as sample and the other electrode as tip, the tunneling current between the sample and the tip is proportional to the tunneling probability and thus has exponential dependence on the tip-sample separation.

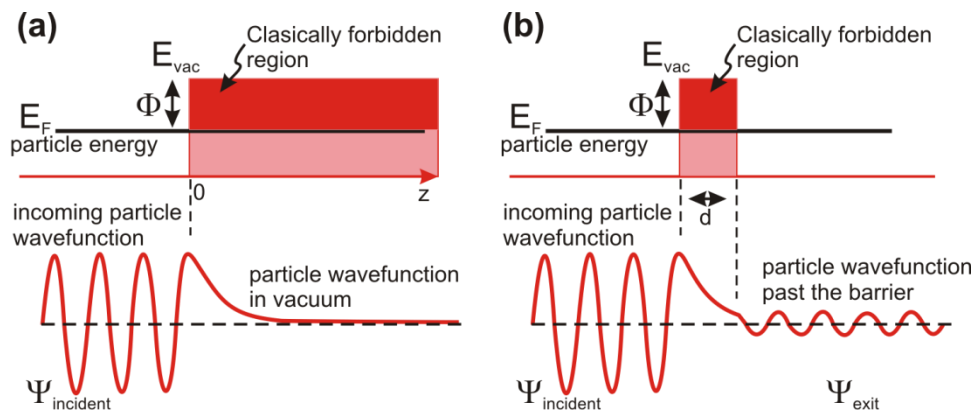


**Fig.3** Top panel: potential diagram for electron in a solid. Lower panel: (a) the exponential decay of the wave-function in the vacuum. (b) Electron wave-function in front of, inside, and behind the barrier.

## 3.2 Tunnelling microscopy and spectroscopy in the STM

### 3.2.1 Transfer Hamiltonian

The tunnelling process in the STM can be understood as a transition from a quasi-stationary state in the tip to a quasi-stationary state in the sample (or vice versa) under the influence of a perturbing Hamiltonian  $\hat{H}_T$ , the transfer Hamiltonian. The transfer Hamiltonian is given by

$$\hat{H} = \hat{H}_{\text{sample}} + \hat{H}_{\text{tip}} + \hat{H}_T$$

For weak coupling between tip and sample, we can interpret  $\hat{H}_0 \equiv \hat{H}_{\text{sample}} + \hat{H}_{\text{tip}}$  as unperturbed Hamiltonian with eigenstates  $\psi_\mu$  in the tip and  $\psi_\nu$  in the sample, and  $\hat{H}_T$  as a weak perturbation (Fig. 4). Applying the result of first order time-dependent perturbation theory (Fermi's golden rule), we obtain for the transition rate

$$\Gamma = \frac{2\pi}{\hbar} |\langle \psi_\mu | \hat{H}_T | \psi_\nu \rangle|^2 g(E)$$

where  $g(E)$  is the density of states in the final state.

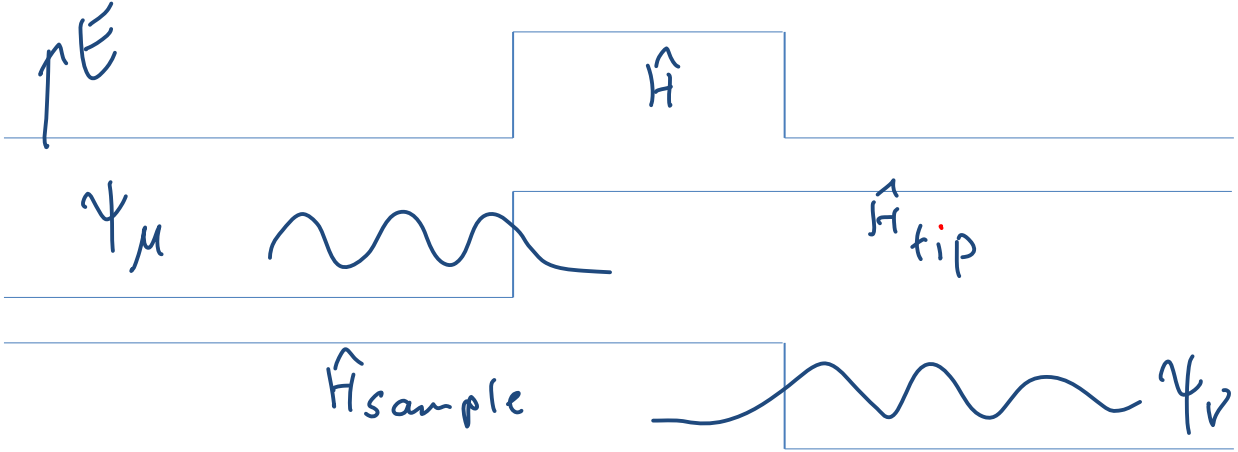


Fig. 4 Potential diagram of the sample (bottom), tip (middle) and the combined system (top). For tip and sample wave functions are also shown.

Following Fermi's golden rule, the tunnelling current can be written as

$$I = \frac{2\pi e}{\hbar} \sum_{\mu,\nu} \{f(E_\mu)[1 - f(E_\nu + eU)] - f(E_\nu + eU)[1 - f(E_\mu)]\} \delta(E_\nu - E_\mu) |\langle \psi_\mu | \hat{H}_T | \psi_\nu \rangle|^2$$

where  $\hat{H}_T$  is the transfer Hamiltonian,  $\psi_\mu$  are states in the tip,  $\psi_\nu$  states in the sample,  $f(E)$  is the Fermi distribution function, and  $U$  the bias voltage (cf. Fig. 5). First term in wavy bracket corresponds to tunnelling from the tip to the sample, the second term to tunnelling from the sample to the tip. According to the above equation, the tunnelling current is therefore proportional to the net total transition rate from states  $\psi_\mu$  to states  $\psi_\nu$ . The matrix element can be written as

$$M_{\mu,\nu} \equiv \langle \psi_\mu | \hat{H}_T | \psi_\nu \rangle = -\frac{\hbar^2}{2m} \int d\vec{S} \cdot (\psi_\mu \vec{\nabla} \psi_\nu - \psi_\nu \vec{\nabla} \psi_\mu),$$

i.e. as the surface integral over the expectation value of the current operator.

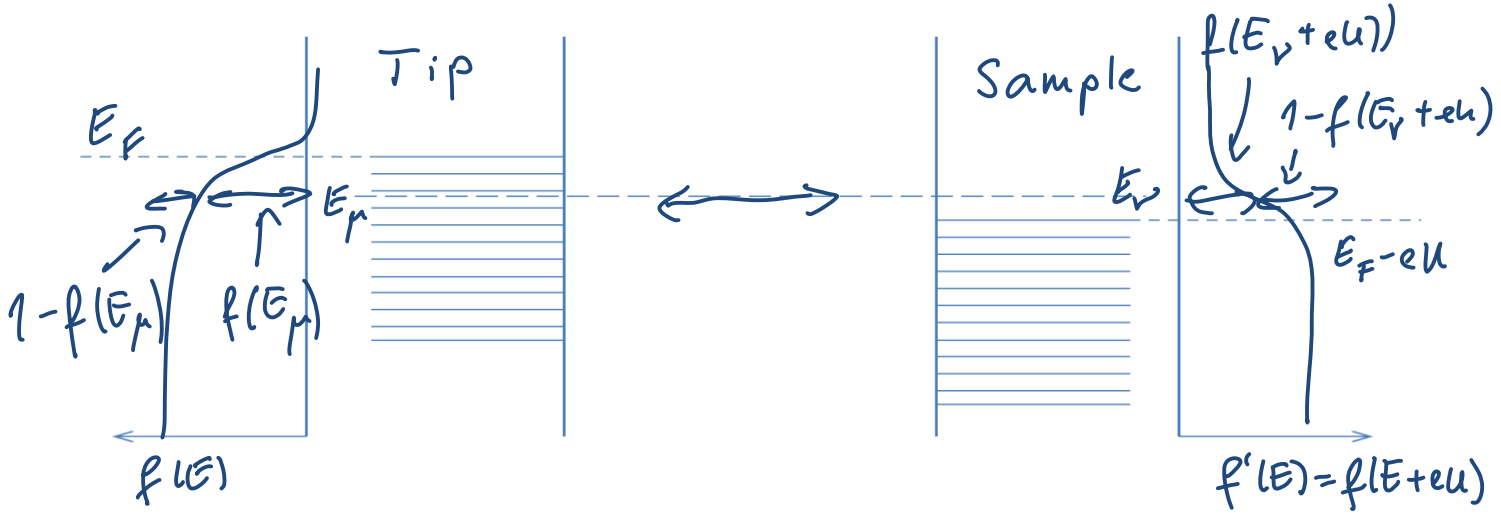


Fig. 5 Energy diagram of the tip and the sample at finite temperature and applied bias to the sample.  $f(E)$  is the Fermi distribution function.

### 3.2.2 Tersoff-Hamann theory

For low temperatures  $T$  and low bias voltages  $U$ , the general expression for  $I$  becomes

$$I = \frac{2\pi e}{\hbar} eU \sum_{\mu,\nu} |M_{\mu,\nu}|^2 \delta(E_{\mu} - E_F) \delta(E_{\nu} - E_F).$$

Within the so-called s-wave approximation we assume that the wave function of the tip has the symmetry of an s-orbital. The current is then described by the famous Tersoff-Hamann formula

$$I \propto \frac{2e^2}{h} U n_t(E_F) e^{2\kappa R} \sum_{\nu} |\psi_{\nu}(\vec{r}_0)|^2 \delta(E_{\nu} - E_F)$$

where  $\frac{2e^2}{h}$  is the quantum of conductance,  $n_t(E_F)$  is the density of states at the Fermi level of the tip,  $\kappa = \sqrt{2m\phi}/\hbar$  is the decay constant,  $\phi$  the effective barrier height, and  $R$  the radius of the tip. The sum on the right hand side of the above equation is the local density of states of the sample at the Fermi energy  $E_F$ , evaluated at the position  $\vec{r}_0$  of the tip, i.e.

$$n_s(E_F, \vec{r}_0) = \sum_{\nu} |\psi_{\nu}(\vec{r}_0)|^2 \delta(E_{\nu} - E_F).$$

Notes:

1. In Tersoff-Hamann theory, we recover “Ohm’s law”, i.e.  $I \propto U$ . However, this is only true in the limit of small  $U$ .
2. For a given barrier height  $\phi$ , a given tip (i.e. given  $n_t(E_F)$ ), and a given bias voltage  $U$ , the tunnelling current is proportional to  $n_s(E_F, \vec{r}_0)$ . This is the *sample quantity* that determines the value of the tunnelling current. The STM thus measures lateral variations of this quantity  $n_s(E_F, \vec{r}_0)$ . In particular, this means that the STM does *not* record a purely topographical signal. Lateral variations in the *electronic* structure also lead to a lateral image contrast, even if there is no variation in topography.

3. The exponential distance dependence of the tunneling current can be recovered from the Tersoff-Hamann result, if it is noted that the sample wave functions  $\psi_v$  decay exponentially into the vacuum,  $\psi_v \propto e^{-\kappa z}$ , i.e.

$$n_s(E_F, \vec{r}_0) \approx n_s(E_F) e^{-2\kappa(s+R)}$$

with  $z = s + R$  ( $s =$  tip-sample distance,  $R =$  tip radius) (Fig.6). Inserting this into the Tersoff-Hamann formula, we obtain

$$I \propto \frac{2e^2}{h} U n_t(E_F) n_s(E_F) e^{2\kappa R} e^{-2\kappa(s+R)} = \frac{2e^2}{h} U n_t(E_F) n_s(E_F) e^{-2\kappa s}.$$

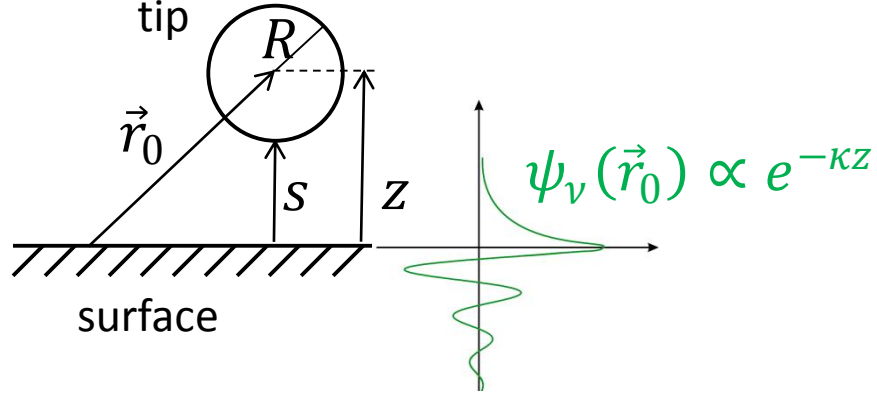


*Fig. 6 Tunnelling model according to Tersoff-Hamann theory with an s shape tip in front of a sample. The diagram on the right indicates electronic states at the surface of the sample.*

4. Extensions of Tersoff-Hamann with other than s-tips show that the so-called ‘derivative rule’ applies:  $x \rightarrow \frac{\partial}{\partial x}$ ,  $y \rightarrow \frac{\partial}{\partial y}$ ,  $z \rightarrow \frac{\partial}{\partial z}$ . For example, with a  $p_z$ -tip orbital, the tunnelling matrix element (and therefore the tunnelling current) is proportional to the  $z$ -derivative of the sample wave function at the centre of the tip apex atom. This means that, generally speaking, other tips than s-tips yield a stronger image corrugation.

### 3.2.3 Tunnelling spectroscopy

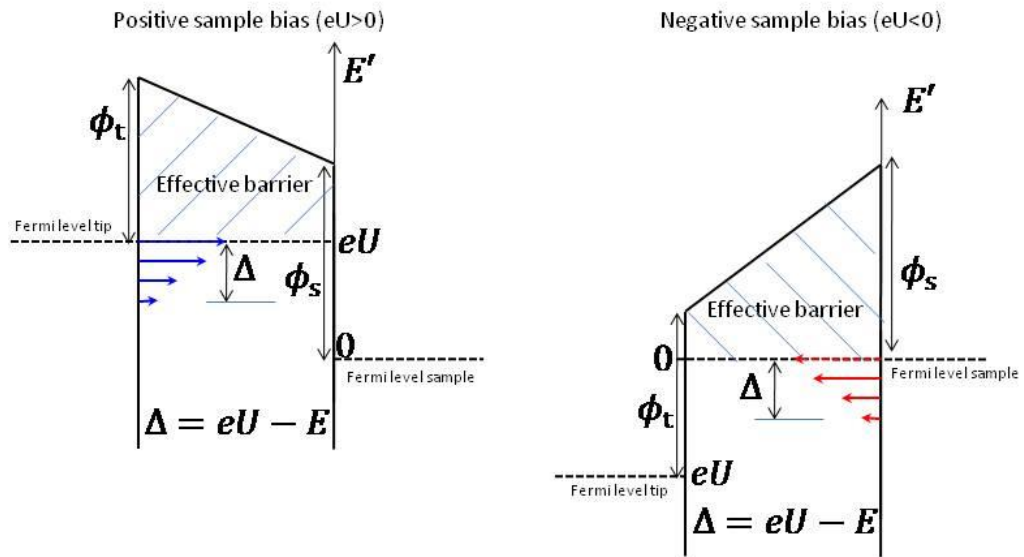
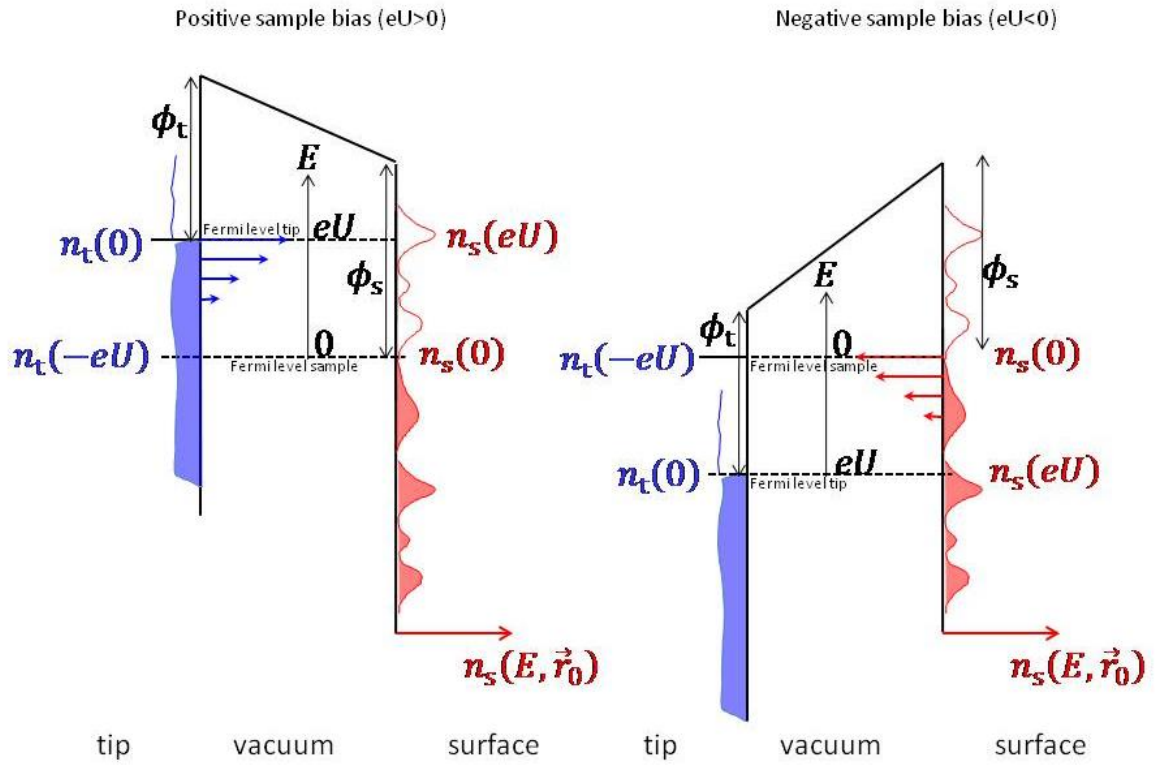
In tunnelling spectroscopy, the bias dependence of the tunnelling current is used to gain additional information about the electronic structure of the sample. Generalizing the Tersoff-Hamann formula to a finite bias window  $eU$ , we obtain

$$I(U) \propto \frac{2e}{h} \int_0^{eU} n_t(-eU + E) n_s(E, \vec{r}_0) e^{2\kappa_{\text{eff}}(E,U)R} dE$$

Note that the decay constant and the barrier height have now acquired an energy and bias dependence (Fig. 7)

$$\kappa_{\text{eff}}(E, U) = \frac{\sqrt{2m\phi_{\text{eff}}(E, U)}}{\hbar}$$

$$\phi_{\text{eff}}(E, U) = \frac{\phi_t + \phi_s}{2} + \frac{eU}{2} - E.$$



$$\phi_{\text{eff}}(E, eU) = \frac{[\phi_t + \Delta] + [\phi_s - eU + \Delta]}{2}$$

Fig. 7 (previous page) Schematic of tunnelling at finite bias. In the upper part densities of states in tip and sample are displayed. In the lower part the effective barrier height for electrons at the Fermi level is shown.

We can also generalize  $n_s(E_F, \vec{r}_0) \approx n_s(E_F)e^{-2\kappa(s+R)}$  to

$$n_s(E, \vec{r}_0) = n_s(E)e^{-2\kappa_{\text{eff}}(E,U)(s+R)}$$

and thus obtain

$$I(U) \propto \frac{2e}{h} \int_0^{eU} n_t(-eU + E) n_s(E) T(E, U) dE$$

with the tunnelling transmission function defined as

$$T(E, U) = e^{-2\kappa_{\text{eff}}(E,U)s}.$$

Notes:

1. The larger the bias, the larger is  $T_{\text{tunnel}}(E, U)$ . The reason is that tunneling is dominated by electrons at  $E_F$  of the negatively bias electrode. For those electrons, an increasing  $U$  will always lead to an effective reduction of the barrier height (Fig. 7). This leads to the following rule of thumb: For each volt of increasing bias the tunneling current increases by one order of magnitude.
2. However, an additional effect comes into play through  $n_s(E)$ . For example, whenever the Fermi level of the negatively biased tip passes a resonance in  $n_s(E)$ , a rapid increase in the tunnelling current will occur. In the differential conductance  $\frac{dI}{dU}(U)$  this will lead to a peak (Fig. 7). Formally, this can be seen by taking the derivative of  $I(U)$ :

$$\frac{dI}{dU}(U) \propto \frac{2e^2}{h} n_t(0) n_s(eU) T(eU, U) + \int_0^{eU} n_t(-eU + E) n_s(E) \frac{dT(E, U)}{dU} dE.$$

This equation shows that on the background that increases non-linearly with  $U$  there will structure superimposed which is directly proportional to the density of states of the sample. This is the basis of (scanning) tunnelling spectroscopy (STS).

## 4 Experimental Technique

### 4.1 Electronic control unit

A schematic of an STM electronic control unit is shown in Fig 8. All the parameters like tunnelling voltage, tunnelling current, piezo voltages etc. can be controlled from the computer software.

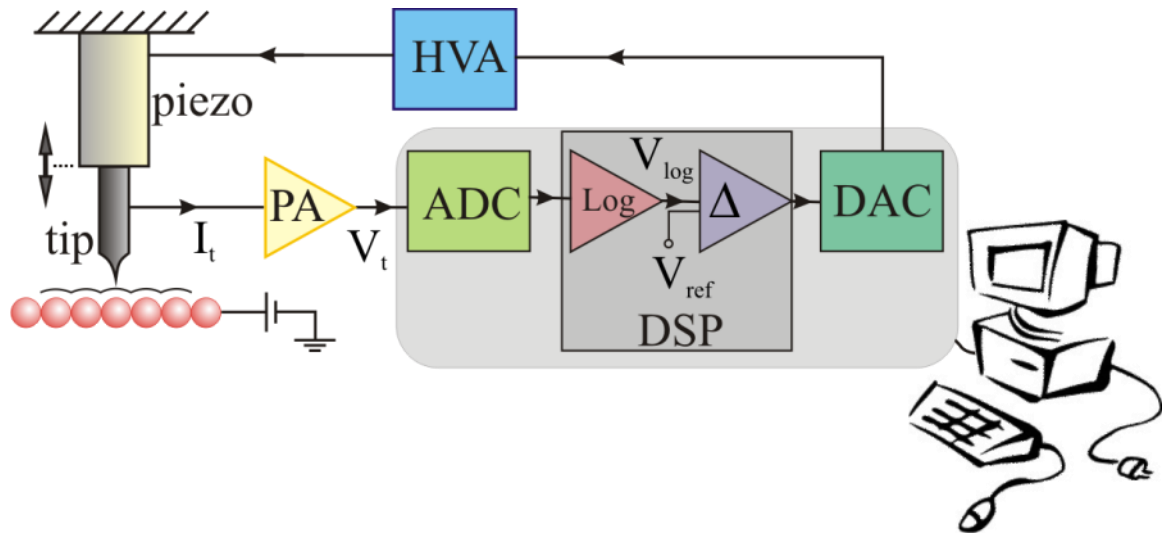


*Fig.8 Schematic of the electronic control circuit for computer-controlled STM data acquisition.*

#### 4.1.1 Current measurement

The tunnelling current in STM is usually very small, in the range of  $\sim 0.01$ - $1$  nA. Therefore, the essential element in the STM electronics is the current amplifier. It amplifies the tunnelling current and converts it into voltage. The gain  $G$  of the current amplifier can be set between  $10^4 - 10^9$  V/A. The resulting voltage is afterwards read by the Analog to Digital Converter (ADC or A/D).

#### 4.1.2 Scanning

Scanning is done by the piezoelectric scanner. Scanning voltages for driving the piezos are generated by the D/A converter. The voltage from the D/A converter (range  $\pm 10$  V) is later amplified by the HV amplifier (the possible gains are  $\times 1$ ,  $\times 3$ ,  $\times 10$ ,  $\times 30$ ) and applied to the piezos. The range of the HV amplifier is  $\pm 200$  V.

The displacement of the piezo  $\Delta l$  at the given applied voltage is defined by the piezoconstant. The scanner is characterized by two piezoconstants: the  $xy$ -piezoconstant and the  $z$ -piezoconstant:

$$\Delta l_{x,y} = d_{x,y} V_{x,y}$$

$$\Delta l_z = d_z V_z$$

The unit of the piezoconstants is  $\text{\AA}/\text{V}$ . Piezoconstants vary with temperature.

#### 4.1.3 Bias voltage

Bias voltage is applied to the sample. If positive voltage is applied to the sample, the electrons tunnel from the tip to the sample. If negative voltage is applied to the sample, the electrons tunnel from the sample to the tip.

#### 4.1.4 A/D and D/A converters

The converters convert digital computer signals to analog voltages and vice versa. They are used to read the tunneling current (converted into voltage by the current amplifier) and apply voltages to piezos. Note that the converters have finite number of steps. The converters used here have a full range of  $\pm 10$  V and an accuracy of 20 Bit. This means that the number of single steps is  $2^{19} + 1$  and the smallest possible voltage step is

$$\frac{10 \text{ V}}{2^{19} + 1} = 19 \mu\text{V}$$

A single step of the converter is called the DAC unit (one DAC unit is equal to  $19\mu\text{V}$ ).

#### 4.2 Constant current imaging

For sample topography measurements the STM operates usually in constant current mode: While the surface is scanned, the vertical position of the tip is adjusted by means of a feedback loop to keep the tunneling current constant (i.e. constant tip sample separation). A topographical map of the sample surface is produced directly from the coordinates of the vertical tip positions for given current.

The feedback loop works as follow: The tunneling current  $I_t$  is amplified by factor  $10^9$  by preamplifier (PA) and converted to a digital voltage  $V_t$  by the Digital to Analog Converter (DAC).  $V_t$  is compared to the set point value  $V_{ref}$ . If the measured current  $V_t$  differs from the set point value  $V_{ref}$ , the electronic control unit adjusts the tip sample separation (by sending an appropriate voltage to the z-piezo by means the Digital to Analog Converter (DAC) and the High-Voltage Amplifier (HVA)) in order to keep the tunnelling current constant. If the measured tunnelling current is larger than the reference current, the tip is retracted from the surface (and opposite: if the tunnelling current is smaller than the reference, the tip is brought closer to the sample). In this way a constant tip-sample separation is established at all  $x,y$ -positions above the sample surface. The  $z(x,y)$ -contour of the tip is displayed on the computer screen as a gray scale image.

#### 4.3 $I(z)$ - spectroscopy

One of the properties of the tunnelling current is that it decays exponentially with the increasing distance between the tip and the sample. The dependence of the current on the distance  $z$  is expressed by

$$I \propto e^{-2\kappa z}$$

If the tunnelling voltage is much smaller than the barrier height,  $\kappa$  is called the decay constant and for small voltages is related to the local barrier height  $\phi$  by

$$\kappa = \frac{\sqrt{2m\phi}}{\hbar}$$

where the local barrier height  $\phi$  is related to the work functions  $\phi_{\text{tip}}$  and  $\phi_{\text{sample}}$  of tip and sample by

$$\phi = (\phi_{\text{tip}} + \phi_{\text{sample}})/2$$

In order to measure the dependence of the tunneling current upon the distance the tip is moved in the  $z$ -direction and simultaneously the tunneling current is recorded. The result is the  $I(z)$  curve. From the plot the decay constant of the current and the local barrier height  $\phi$  can be determined.

In literature,  $\phi$  measured in this way is often called ‘apparent work function’ or ‘apparent barrier height’. Its experimental value varies with the applied voltage and tip-sample distance and also depends on the work function of the tip.

#### **4.4 Differential conductance spectroscopy**

In chapter 2.3.2 it was already mentioned that the differential conductance is directly proportional to the density of states of the surface. Therefore it is interesting to measure the first derivative of the tunneling current. For this a lock-in-amplifier is used, which allows to measure with a high signal to noise ratio. The only requirement is that the measured signal oscillates with a fixed frequency and phase. Under these conditions it is even possible to detect a signal, when the overall noise level is higher than the signal itself.

A lock-in-amplifier measures by multiplying the input signal with an internal reference signal. For the multiplication of two harmonic signals one finds

$$A\cos(\omega_1 t + \varphi) \times B\cos(\omega_2 t) = \frac{1}{2}AB\{\cos[(\omega_1 + \omega_2)t + \varphi] + \cos[(\omega_1 - \omega_2)t + \varphi]\}$$

where  $\omega_1$  and  $\omega_2$  are the frequencies of the two signals, A and B are their amplitudes and  $\varphi$  is the phase difference between the signals. If  $\omega_1 = \omega_2 = \omega$  the product signal results in a DC component  $\frac{1}{2}AB\cos(\varphi)$  plus a harmonic signal which oscillates with  $\omega$ . By integrating the signal over a certain time the harmonic component vanishes and only the DC part prevails which is proportional to the amplitudes of both signals.

To measure the first derivative of the tunneling current with the lock-in-amplifier the reference signal is directly added to the bias.

$$U_{sample} = U_{bias} + U_{lock\ in} \cos(\omega t).$$

This results in an oscillation of the tunnelling current at the same frequency as the reference signal. The amplitude with which the current oscillates is proportional to its first derivative and can be easily detected by the lock-in-amplifier. A schematic view of this relation between input and output signal for different bias is shown in fig. 9.

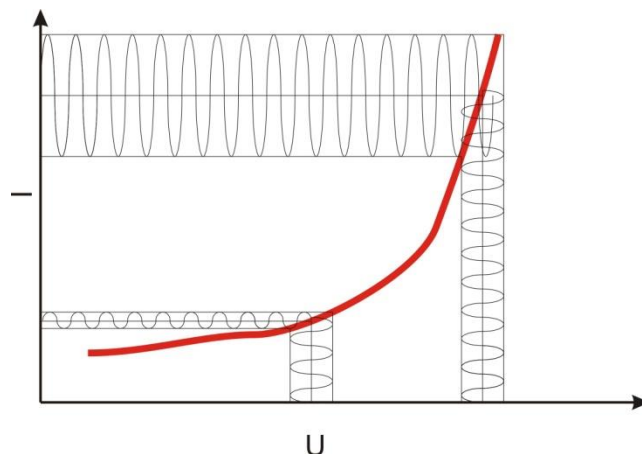


*Fig.9 Measurement of the differential conductance of the tunnelling current with the lock-in-technique. The amplitude of the modulated tunnelling current is proportional to the slope of the I(V) curve.*

The lock-in-technique also allows measuring higher derivatives, when higher harmonics of the reference signal are used.

## 5 Sample

The system under investigation during the experiment is the organic molecule PTCDA adsorbed on the Ag (111) surface. The metal surface is prepared by repeated cycles of  $\text{Ar}^+$  sputtering and temperature annealing at  $550^\circ\text{C}$ . On the clean surface, a submonolayer of molecules is deposited at 100 K temperature from a home-built evaporator. The deposition rate is 0.1 monolayer per minute at  $300^\circ\text{C}$  of the evaporator. Further the sample is annealed at 200K for 1 minute. After the deposition the sample is cooled to  $\text{LN}_2$  temperature on the manipulator before loading into the STM.

On the Ag(111) surface PTCDA molecules are chemisorbed and form ordered islands in a so called herringbone structure. An example for this ordered structure can be found in fig. 10b.

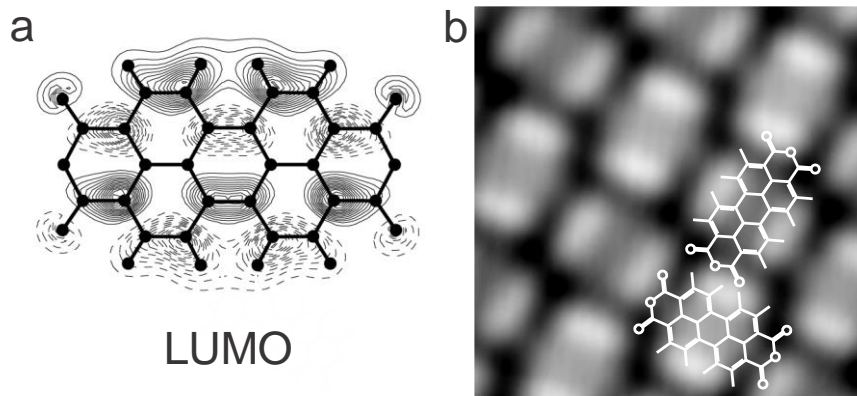


*Fig.10 a) ball and stick model of a PTCDA molecule shown together with the electron density distribution corresponding to the Lowest Unoccupied Molecular Orbital (LUMO). Note that it is the LUMO of PTCDA that mostly contributes to the imaging contrast obtained with the STM b) image of a PTCDA layer on Ag(111) at  $U_{bias} = -0.34V$*

## 6 Tasks

### 6.1 Piezo calibration

To measure the distances and heights in STM, you need to know the piezoconstants. Normally the piezoconstants of the STM scanner have to be calibrated. What may be the way to do the calibration of the piezoconstants? Try to determine the XY and Z-piezo constant of the STM from the STM images of the Ag(111) surface.

*Hint: The height of a single step on Ag(111) surface is 2.89 Å. The unit cell of the PTCDA/Ag(111) is  $18.96 \times 12,61$  Å.*

### 6.2 Constant current imaging

You already recorded several images, now search for a nice patch of PTCDA molecules and try to image them at different bias voltages. What is the difference in the images if you go for example from negative to positive bias? You can also try to image the edge of an island and repeat the measurements again. What do you observe?

*Note: During the experiments you should not exceed  $\pm 2$  V; otherwise you might damage the molecules in the layer.*

### 6.3 Current-distance spectroscopy

Show that the tunneling current changes exponentially with distance between the tip and the sample. Analyze the curves to determine the decay constant  $\kappa$  of the current on Ag(111). From the decay constant calculate the work function of Ag(111).

*Hint: To analyze the curves properly remember to convert the tunneling current and Z-position into proper units (Convert current to nA and Z-position to Å)!*

## 6.4 Differential conductance spectroscopy

Measure the differential conductance with the lock in technique. Are there differences in the spectra for different positions on the molecule and maybe also differences for different molecules inside the layer?

*Hint: You should measure again between  $\pm 2V$ . To convert the output of the lock in amplifier into physical values you should compare this value with the simultaneously measured tunneling current. Usually the differential conductance is either given in Siemens (S) or in units of the quantum of conductance ( $G_0$ ).*

## 7 Literature

C.J. Chen, *Introduction to Scanning Tunneling Microscopy*, Oxford University Press, New York, 2007.

J.A. Stroscio, W.J. Kaiser, *Scanning Tunneling Microscopy*, Academic Press, San Diego, 1993.

E. Meyer, H.J. Hug, R. Bennewitz, *Scanning Probe Microscopy*, Springer, 2003

F.S. Tautz, *Structure and bonding of large aromatic molecules on noble metal surfaces: The example of PTCDA*, Progress in Surface Science **82**, 479-520, 2007

R. Wiesendanger, *Scanning Probe Microscopy and Spectroscopy: Methods and Applications*, Cambridge University Press, 1994